Collisional removal of O_2 ($c\ ^1\Sigma_u^-$, v=9) by O_2, N_2, and He

Richard A. Copeland, Karen Knutsen,[a] Marc E. Onishi, and Talat Yalçin[b]
SRI International, Molecular Physics Laboratory, Menlo Park, California 94025

(Received 20 August 1996; accepted 13 September 1996)

The collisional removal of O_2 molecules in selected vibrational levels of the $c\ ^1\Sigma_u^-$ state is studied using a two-laser double-resonance technique. The output of the first laser excites the O_2 to v=9 or 10 of the $c\ ^1\Sigma_u^-$ state, and the ultraviolet output of the second laser monitors specific rovibrational levels via resonance-enhanced ionization. The temporal evolution of the $c\ ^1\Sigma_u^-$ state vibrational level is observed by scanning the time delay between the two pulsed lasers. Collisional removal rate constants for $c\ ^1\Sigma_u^-$, v=9 colliding with O_2, N_2, and He are $(5.2\pm0.6)\times10^{-12}$, $(3.2\pm0.4)\times10^{-12}$, and $(7.5\pm0.9)\times10^{-12}$ $cm^3\ s^{-1}$, respectively. As the rate constants for O_2 and N_2 are similar in magnitude, N_2 collisions dominate the removal rate in the earth's atmosphere. For v=10 colliding with O_2, we find a removal rate constant that is 2–5 times that for v=9 and that single quantum collision cascade is an important pathway for removal. © *1996 American Institute of Physics.* [S0021-9606(96)02847-4]

I. INTRODUCTION

When two oxygen atoms recombine in a collision with a third body, a significant fraction of the formed oxygen molecules lie in one of the three *ungerade* electronic states near the dissociation limit.[1] This cluster of two triplet states ($A\ ^3\Sigma_u^+$, $A'\ ^3\Delta_u$) and one singlet state ($c\ ^1\Sigma_u^-$) is often called the Herzberg states of O_2 because of his pioneering work in their spectroscopy.[2] Their potential energy curves, and those of other low-lying states of O_2, are shown in Fig. 1. In this laboratory we have begun a comprehensive study of collisional processes involving O_2 molecules in the Herzberg states, motivated by their importance to the nightglow of planetary atmospheres.[3–6]

In the earth's upper atmosphere (85–110 km), nightglow emission in the ultraviolet and blue spectral regions is observed from all three Herzberg states. These states, produced by three-body recombination of oxygen atoms in the atmosphere, are metastable: there are no allowed electronic transitions either among the Herzberg states, or from them to any of the three lower-lying O_2 electronic states ($b\ ^1\Sigma_g^+$, $a\ ^1\Delta_g$, and $X\ ^3\Sigma_g^-$). Because of their long radiative lifetimes,[7] collisions play a dominant role in their emission intensities, even though atmospheric pressures at the relevant altitudes are low (about 1 mTorr at 100 km). The $A\ ^3\Sigma_u^+ - X\ ^3\Sigma_g^-$ electronic transition (Herzberg I) is the dominant emission from the Herzberg states in the earth's atmosphere, but the $c\ ^1\Sigma_u^- - X\ ^3\Sigma_g^-$ (Herzberg II) and $A'\ ^3\Delta_u - a\ ^1\Delta_g$ (Chamberlain) transitions have also been identified.[8] Currently, identification of the $A'\ ^3\Delta_u - X\ ^3\Sigma_g^-$ (Herzberg III) emission in the earth's atmosphere is still tentative.[9,10] For all three Herzberg states, emission originates from excited vibrational levels, with the maximum emission intensity coming from v=4–7, 5–8, and 5–10 for the $A\ ^3\Sigma_u^+$, $A'\ ^3\Delta_u$, and the $c\ ^1\Sigma_u^-$ states, respectively.[11]

In sharp contrast to these terrestrial observations, the Herzberg II system dominates the Herzberg state emission in the Venusian nightglow, as observed by the Venera probe.[12] The upper state of the Herzberg II transition, $c\ ^1\Sigma_u^-$, is the lowest energy state of the three, and emission measurements suggest that, not only does the Venusian atmosphere exhibit a strikingly different distribution of the O_2 Herzberg state populations, but emissions originate almost exclusively from the v=0 levels. The CO_2 atmosphere on Venus and the O_2 and N_2 atmosphere on earth create very different spectral signatures, while no O_2 Herzberg state emission has been observed on Mars.[12] Clearly, the collisional environment is critical to determining the spectral characteristics of the emissions. To model these emissions, therefore, collisional rate constants are required for all the important colliders with many of the excited vibrational levels in the Herzberg states. Knowledge of the pathways for relaxation is also crucial to understanding O_2 and O atom emissions on earth and the other planets. The $c\ ^1\Sigma_u^-$ state, in particular, has been implicated as a possible source for the O(^1S) emission in the earth's atmosphere.[13,14]

Our earlier work focused on selected vibrational levels of the $A\ ^3\Sigma_u^+$ state and measured removal rate constants for the important atmospheric colliders.[3,4] A similar experimental approach is applied in this $c\ ^1\Sigma_u^-$ state study. We use the output of one laser to excite ground state O_2 molecules via a "forbidden" one-photon transition to a selected vibrational level of the $c\ ^1\Sigma_u^-$ state, and then use the output of a second laser to resonantly ionize only molecules in that excited vibrational level. By varying the time delay between the two laser pulses, we obtain the temporal evolution of the excited level. The strong bands of the $c\ ^1\Sigma_u^- - X\ ^3\Sigma_g^-$ transition are about 20 times weaker than those of the $A\ ^3\Sigma_u^+ - X\ ^3\Sigma_g^-$ transition, making the excitation more difficult than the previously studied $A\ ^3\Sigma_u^+$ state.[7]

The $c\ ^1\Sigma_u^-$ state has seldom been studied in the laboratory. The 1983 study of Kenner and Ogryzlo is the only

[a]Present address: Battelle Pacific Northwest National Laboratory, P.O. Box 999, MX K2-14, Richland, Washington 99352.
[b]Present address: Department of Chemistry, University of Alberta, Edmonton, Alberta T6G 2G2, Canada.

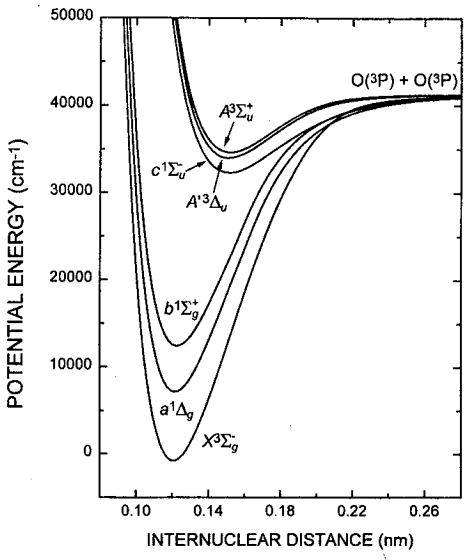

FIG. 1. Potential energy diagram for the Herzberg and lower-lying states of O_2.

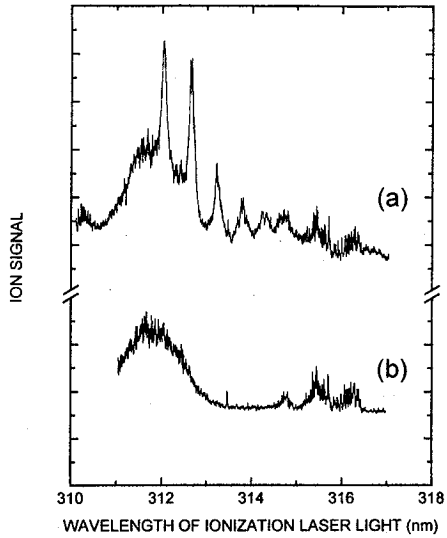

FIG. 2. O_2 ion signal as a function of the wavelength of the ionization laser light at an oxygen pressure of 15.5 Torr. The delay between the excitation and ionization laser pulses is approximately 50 ns. The top curve, labeled (a), shows the ion signal when the excitation laser light at 261.245 nm populates the J=14, v=9 level of the $c\ ^1\Sigma_u^-$ state. The bottom curve, labeled (b), shows the ion signal when the light is tuned out of resonance with the $c\ ^1\Sigma_u^- - X\ ^3\Sigma_g^-$ transition. The features in the bottom curve are due to ionization of O_2 molecules in the ground electronic state.

previous laboratory study to extract quantitative rate constants for the $c\ ^1\Sigma_u^-$ state.[15] Using a nickel surface to enhance the production of excited electronic states of O_2 in a microwave discharge flow tube, they extracted removal rate constants for the lowest lying vibrational level with the colliders $O(^3P)$, O_2 ($a^1\Delta_g$), O_2, CO_2, SF_6, N_2O, He, and Ar.[15] These measurements are directly applicable to the atmosphere of Venus, where emission from v=0 dominates, but are less applicable to the terrestrial atmosphere, where emission from higher vibrational levels is important. In those experiments, many excited electronic states were produced at the Ni surface, and the accuracy of the measurements has been questioned due to the possibility of cascading and other complications.[16] Rate constants have also been extracted from nightglow observations,[16–19] and have been consistently much larger than those obtained from the laboratory work of Kenner and Ogryzlo.[15] Clearly, more laboratory work is needed to understand these discrepancies.

II. EXPERIMENTAL APPROACH AND RESULTS

In brief, ground-state O_2 molecules are excited to specific ro-vibronic levels in the $c\ ^1\Sigma_u^-$ state by direct, pulsed-laser excitation in a room temperature flow cell containing only O_2, or O_2 and a collision partner. A time-delayed second pulsed laser monitors the temporal evolution of the excited molecules via a newly developed resonance-enhanced ionization technique. We fit the signal intensity as a function of time delay between the lasers, and by varying the O_2 and collider pressures, extract the total removal rate constant for a specific vibrational level. A detailed description of the experimental apparatus can be found elsewhere;[4] here we focus on the unique aspects of this investigation.

A. Resonance enhanced ionization probing of the $c\ ^1\Sigma_u^-$ state

Key to our experimental approach is the development of a pulsed laser method to specifically probe selected vibrational levels of the $c\ ^1\Sigma_u^-$ state. The fraction of $c\ ^1\Sigma_u^-$ state molecules that fluorescence under typical laboratory conditions is so small that waiting for emission is not feasible. Instead, a newly developed resonance-enhanced ionization technique similar to that used for detection of the $A\ ^3\Sigma_u^+$ state is the preferred approach.[3,4]

Initially, we observed resonance-enhanced ionization features of the $c\ ^1\Sigma_u^-$ state in an indirect manner, by examining the pathways for $A\ ^3\Sigma_u^+$ state removal. In these experiments, we prepared O_2 molecules in the $A\ ^3\Sigma_u^+$ v=8 level and recorded the ionization spectrum at several delay times between the excitation and probe laser pulses. We examined the energy region below the 2+1 ionization threshold of ground state $O_2(\lambda>306$ nm), thus avoiding the interference of ionization from the ground state. After a long delay (270 ns at 22.5 Torr) between the laser pulses, several strong, broad features appeared in the ionization spectrum. We assigned these features to O_2 ionized out of vibrationally excited levels (v=9, 10, and 11) of the $c\ ^1\Sigma_u^-$ state. To confirm this identification, we excited O_2 directly to the $c\ ^1\Sigma_u^-$ state thus demonstrating that these ionization features appeared promptly and at the same photon energies, as in the initial experiment described above.

Figures 2(a) and 3(a) show the ionization spectra following excitation of the v=9 and 10 vibrational levels of the $c\ ^1\Sigma_u^-$ state, respectively, on top of the background ionization of O_2 caused by the ionization laser alone. The energies

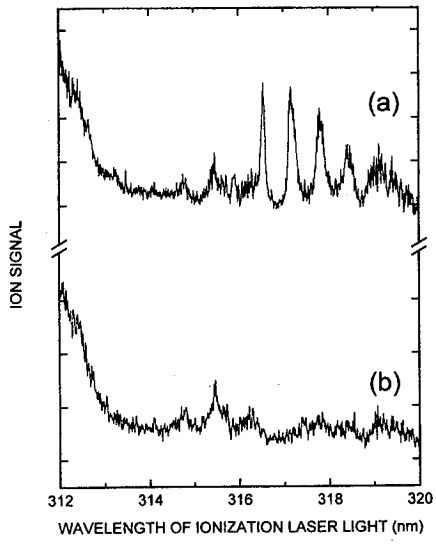

FIG. 3. O_2 ion signal as a function of the wavelength of the ionization laser light at an oxygen pressure of 10.1 Torr. The delay between the excitation and ionization laser pulses is approximately 45 ns. The top curve, labeled (a), shows the ion signal when the excitation laser light at 257.137 nm populates the J=6 and 10, v=10 levels of the $c\ ^1\Sigma_u^-$ state. The bottom curve, labeled (b), shows the ion signal when the light is tuned out of resonance with the $c\ ^1\Sigma_u^- - X\ ^3\Sigma_g^-$ transition. The features in the bottom curve are due to ionization of O_2 molecules in the ground electronic state.

for the Herzberg II transitions are well known,[20] so we can be certain of the vibrational and rotational level or levels we are populating with the excitation laser. Figures 2(b) and 3(b) are taken with the excitation laser off-resonance with the $c\ ^1\Sigma_u^-$ state or any other O_2 Herzberg transition. They show only a background ionization of ground-state O_2 due to the probe (ionization) laser. These spectra are independent of the wavelength of the excitation laser and, in fact, are the same even if the excitation laser is turned off. In these off-resonance spectra, we see a broadband between 311 and 313 nm, assignable to ionization out of v=1 of the ground electronic state by way of the lowest vibrational level of the first Rydberg state, $C\ ^3\Pi_g$. At room temperature, about 0.04% of O_2 molecules lie in the v=1 level. This band is broad due to predissociation in this Rydberg state vibrational level,[21] and provides a good benchmark for the other features observed below. The two sharp features near 313.4 and 313.9 nm in Fig. 2(b) are not observed above the noise in Fig. 3(b), and may be due to multiphoton ionizations that are extremely power dependent. The three groupings between 314.5 and 316.5 nm are currently unidentified, but are reproducible from spectrum to spectrum. These features are more sensitive to the laser pulse energy than the band near 312 nm, therefore, we conclude they are due to a process involving more photons, perhaps a 3+1 ionization. A one-photon absorption spectrum of O_2 shows many bands in this same energy region,[22–24] and a three-photon transition can access similar electronic states. However, in the recent absorption work of England *et al.*,[24] the features they assign in this energy region do not correspond to those we measure here. Thus, multiphoton features could be a direction for future investigations of O_2 Rydberg state spectroscopy.

In Fig. 2(a), new, strong features are observed at short delay times when the v=9 level of the $c\ ^1\Sigma_u^-$ is populated. Most significant are the two features near 312 and 312.7 nm. These are much broader than the laser linewidth [which can be estimated from the lines near 316 nm in Fig. 2(b)]. We expect that the increased width is due to a predissociation in the state that resonantly enhances the ionization. If this is really ionization of v=9, then when we excite to v=10 of the $c\ ^1\Sigma_u^-$ state, these features should move to longer wavelengths, if the same intermediate states are accessed. This phenomenon is observed in Fig. 3(a). Although the relative intensities change somewhat, the general structure of the ionization features agree in both spectra, Fig. 2(a) and Fig. 3(a), and the positions are redshifted in Fig. 3(a) by the spacing between the v=9 and 10 levels of the $c\ ^1\Sigma_u^-$ state. Thus, the vibrational level origin of these features is verified even though the exact assignment of the intermediate state has not been established as yet. We can now use these features as a "fingerprint" for detection of v=9 and 10, and for monitoring their temporal evolution. Several subtle rotation-specific effects of using these ionization paths will be presented in the analysis of the time-dependent data.

B. The $c\ ^1\Sigma_u^-(v=9)$ removal measurements

The bulk of the time-dependent data is taken with excitation to v=9, J=2, and 6 via the overlapped $^RQ(5)$ and $^PQ(3)$ lines, followed by ionization at 312 nm.[20] Typically the data are obtained with 10 ns resolution near the peak of the signal and with 40 ns resolution at longer time delays, averaging 35 laser pulses at each delay. The pressure in the system is kept constant during data acquisition. Data are obtained by doing an on-resonance, off-resonance subtraction under identical collision conditions. Typical experimental data are shown in Fig. 4.

For the removal measurements with O_2 as the collider, we vary the pressure between 5 and 35 Torr. At high pressures, we are limited by our ability to collect the ions. At low pressures, the ionization background becomes more intense, and diffusion out of the overlap region of the two laser beams becomes significant. Initially, we attempted to fit the experimental data to a single exponential, as shown in Fig. 4 by the dashed line. Clearly, there are systematic differences between the experimental data and the single exponential fit, both at short and long delay times. The data appear to fall more rapidly at small time delays, and the rate of decrease is smaller at longer delay times when compared to the single exponential approximation. This results in the single exponential fit crossing the experimental data twice. The solid line is a two-exponential fit to the data, which, naturally, does a significantly better job than a single exponential at approximating the dependence of the signal intensity on the time delay between the two lasers. Systematic differences at both short and long delays are significantly reduced. The difference in the two exponential decay constants in the double exponential fit is approximately a factor of 8 at 15

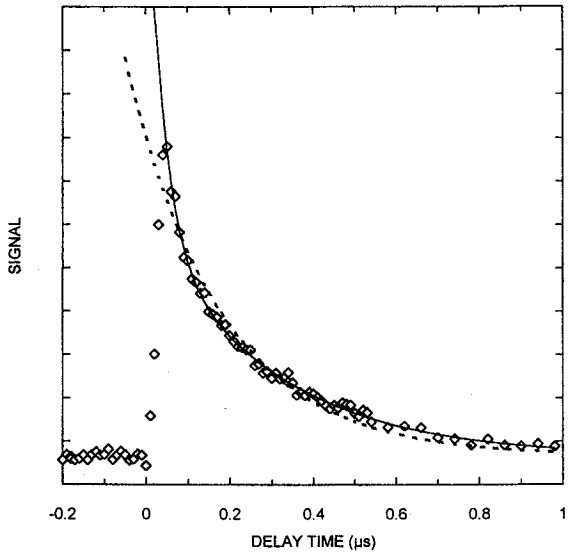

FIG. 4. O_2 v=9 ion signal as a function of delay between the two laser pulses at 15 Torr. The diamonds are the experimental data points, the dashed line is the best-fit single exponential decay, and the solid line is the best fit using two exponentials.

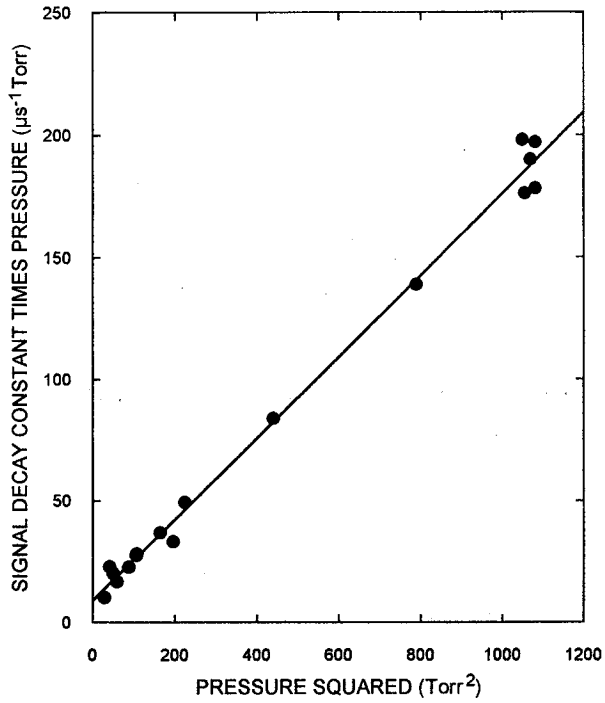

FIG. 5. Plot of the decay constant times pressure versus pressure squared for O_2 ($c\ ^1\Sigma_u^-$, v=9) colliding with O_2. The circles are the experimental data and the solid line is the linear least squares fit to that data. The slope gives the collisional removal rate constant and the y intercept is an effective rate for diffusion of the $c\ ^1\Sigma_u^-$ molecules out of the observation region.

Torr. If we restrict the single exponential fit to longer delay times (>0.3 μs), we obtain a decay constant value similar to the value of the slower exponential from the double exponential fit. We attribute the rapid exponential to rotational equilibration out of the ionized rotational level in the $c\ ^1\Sigma_u^-$ state, and the slower exponential to the removal of the rotationally equilibrated excited vibrational level in the $c\ ^1\Sigma_u^-$ state. Of course, the rotational equilibration process cannot be assigned to a single exponential, but approximating it as such is a convenient way to extract the slower exponential, and has little effect on the magnitude of the slower exponential.

Several experimental tests examine the rotational equilibration process and demonstrate that the slow exponential is indeed due to molecules leaving the rotational equilibrated v=9 level. These experiments also help us to understand the origin of the ionization spectra seen in Figs. 2 and 3. We excite different rotational levels between N=2 and 18, and monitor the relative magnitude of the fast and slow exponentials from the double-exponential fit, along with any changes in the slow exponential or the ionization spectrum. If this double exponential is a rotational level effect, we expect the relative contributions of the two exponentials to change, and perhaps also the rate for the fast exponential, but the rate for the slow exponential should remain constant. We find that the relative contribution of the fast exponential increases as we increase the rotational quantum number of the $c\ ^1\Sigma_u^-(v=9)$ state, over the range of rotational levels given above. In addition, the fast exponential decay rate increases with increasing rotational level over this range. From these observations, we conclude that in our removal experiments, we are ionizing out of high rotational levels in the $c\ ^1\Sigma_u^-$ state, and the two-exponential behavior is consistent with a transient overpopulation of the ionized rotational level as the O_2 molecules move through it on the way to equilibrium. We conclude that the ionization spectrum originates exclusively from high rotational levels for both v=9 and 10. Only a few selected rotational levels in the intermediate state live long enough to act as a stepping stone to ionization, since the entire vibrational band does not appear in the ionization spectrum. This hypothesis is supported by the insensitivity of the wavelength dependence of the ionization spectra in Figs. 2 and 3 to the specific excited rotational level. Further experiments are under way to completely assign the rotational level or levels resulting in ionization, and to identify the intermediate state among several possible electronic states.

Figure 5 shows the data for collisional removal of $c\ ^1\Sigma_u^-(v=9)$ in pure O_2. The data are plotted as the product of the decay constant for the slow exponential and the O_2 pressure versus the O_2 pressure squared. A plot of this type is required, since diffusion contributes significantly to the observed signal decay at low pressures. The signal decay constant can be approximated by

$$\tau^{-1} \cong kP + D/P,$$

where τ^{-1} is the best-fit signal decay constant for the slow exponential, P is the pressure of O_2, k is the total vibrational level removal rate constant, and D is an effective diffusion constant for the experimental conditions.[4] The slope of Fig. 5 yields the rate constant for removal of the v=9 level, and the intercept yields the diffusion constant. The rate constant extracted from the slope is given in Table I, along with the

TABLE I. Collisional removal rate constants, k, and thermally averaged cross sections, σ, for the v=9 level of the $c\ ^1\Sigma_u^-$ state.[a]

Collider	k ($cm^3\ s^{-1}$)	σ (Å^2)
O_2	$(5.2\pm0.6)\times10^{-12}$	0.83±0.10
N_2	$(3.2\pm0.4)\times10^{-12}$	0.49±0.06
He	$(7.5\pm0.9)\times10^{-12}$	0.57±0.07

[a]All error estimates are two standard deviations.

thermally averaged collision cross section obtained by dividing the rate constant by the average velocity. In Fig. 5, the cluster of points near 1000 on the abscissa correspond to exciting different rotational levels or probing different ionization features. No statistically significant differences are observed in the slow exponential decay constant by varying these wavelengths. The diffusion constant, D, extracted from the intercept is $9\pm4\ \mu s^{-1}$ Torr. This value is about a factor of 3 larger than those obtained in previous studies of the $A\ ^3\Sigma_u^+$ state of O_2.[4] This difference, perhaps due to a change in laser beam geometry, does not have a large impact on the magnitude of the rate constants. Neglecting diffusion, the extracted rate constant decreases by less than 25%. The error estimate (given in Table I) is two standard deviations of a linear fit of the graph in Fig. 5, added in quadrature with a 10% error for the approximate diffusion correction.

Figure 6 shows the experimental values for the corrected decay constant for the colliders N_2 and He versus collider partial pressure. The points in the figure are extracted from experimental data in which a mixture of O_2 and the collider flow through the cell. The partial pressures of the two components are obtained by measuring the mass flow of each species, separately and the total pressure. Knowing the partial pressures of both O_2 and the collider, together with the value for the decay constant for the slow exponential from the measured signal, we can remove the contribution due to O_2 from the total decay constant. This contribution is calculated using the rate constant given for O_2 in Table I. The diffusion component is also subtracted, assuming that the diffusion constant is the same as determined for pure O_2. This should be a good approximation for the N_2 collider, but will be less accurate for He, where, fortunately, the diffusion correction has a smaller influence. The values of the rate constant, obtained from the slopes of the linear best-fit lines, are given in Table I, along with the thermally averaged cross sections. If we include no diffusion correction, the magnitude of the rate constants decreases by less than 10% for He and less than 20% for N_2. The error estimates are two standard deviations of a linear fit to the data shown in Fig. 6, added in quadrature with a 10% error for the approximate diffusion correction. The extracted rate constant for He is the largest of the three studied colliders, with O_2 being intermediate and N_2 the smallest.

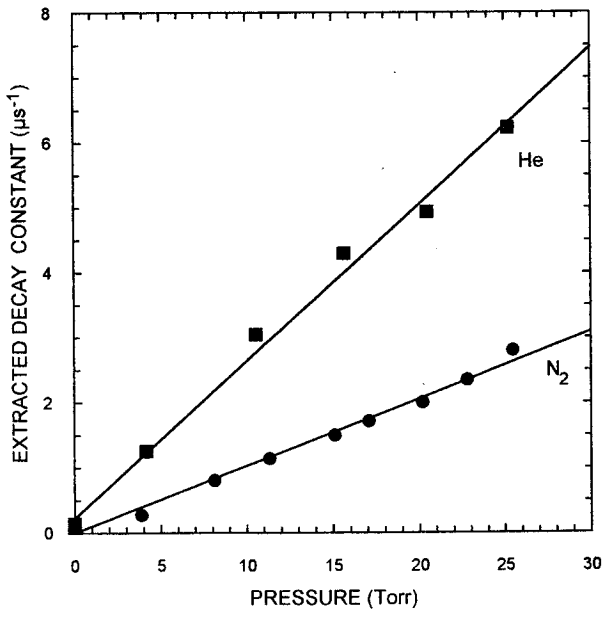

FIG. 6. Plots of the corrected decay constant versus pressure for collisions of O_2 ($c\ ^1\Sigma_u^-$, v=9) molecules with He and N_2. The squares are the He data and the circles are the N_2 data. The solid lines are linear least squares fits to the experimental data.

C. The $c\ ^1\Sigma_u^-(v=10)$ removal measurements

As shown in Fig. 3, we can probe the v=10 level of the $c\ ^1\Sigma_u^-$ state by increasing ionization laser wavelength, and excite to v=10 by increasing the photon energy of the excitation laser light. We observe that, at the same pressure, the signal for v=10 decays significantly faster than does v=9. This observation is independent of the ionization laser wavelength, as shown by measurements on the 316.5, 317.1, and 317.8 nm features in Fig. 3(a). It also did not show a significant dependence on the specific rotational level that was excited in v=10. Just as in the v=9 case, our attempts to fit the data are complicated by the same rotational equilibration effects. However, for v=10 with O_2, the difference between the rotational equilibration process and the removal of the vibrational level is about a factor of 2 versus the factor of 8 observed for v=9. Because of the similarity in the rates of the two processes, separation of the signal decay into rates for the two energy transfer processes is difficult. In addition, vibrational cascading, as shown in Fig. 7, can cause subtle baseline effects in the data, due to ionization of molecules in the v=9 level of the $c\ ^1\Sigma_u^-$ state at the wavelength that detects primarily the v=10 level. From the temporal evolution of the data, we estimate that the v=10 removal rate constant is about a factor of 2–5 times greater than for v=9, with a value between 3 and 4.5 times larger being the most likely. Further experiments are under way to extract accurate, quantitative values. The available data conclusively show that the rate constant does increase going from v=9 to 10.

Information on the v=10 removal can be extracted either from ionizing that level itself (as described above) or by looking at the time dependence of the signal from the v=9 level. The top curve in Fig. 7 shows the v=9 ionization signal following excitation of v=10. The bottom curve shows the v=9 signal following v=9 excitation under the same experimental conditions. The top curve clearly shows a

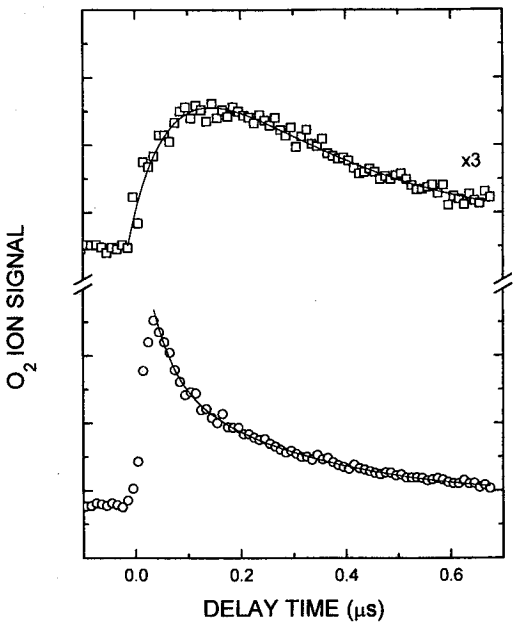

FIG. 7. The v=9 ion signal as a function of time delay between the excitation and ionization lasers following excitation of the v=10 level (top) and the v=9 level (bottom). The top curve has been multiplied by a factor of 3. Both signals were obtained at 15 Torr of O_2.

rise and a fall indicative of a vibrational cascade filling the v=9 vibrational level from v=10. The fall of the signal on exciting v=10 is fit well by the rate for v=9 removal. The solid lines show the fit to the experimental data, with the v=9 removal rate fixed at the value that fits the bottom curve. For this specific pressure, the rising exponential in the top panel is approximately four times the value for v=9 removal in the bottom panel. From the relative intensities of both signals, we conclude single quantum vibrational cascade is a significant removal pathway (>20% for v=10). Further work is under way to make this comparison quantitative. Thus far, only collisions with O_2 have been examined for v=10.

III. DISCUSSION

Since our measurements are the first for the collisional removal of O_2 molecules in vibrationally excited levels of the $c\ ^1\Sigma_u^-$ state, we cannot compare these results directly to any other experimental investigation. The only previous energy transfer experiment on the $c\ ^1\Sigma_u^-$ state was the surface recombination study by Kenner and Ogryzlo, described in Sec. I. They generated removal rate constants for the v=0 level with O_2 and He, among other colliders.[15] The collider N_2 was not investigated. In Table II, we compare our rate constants for v=9 and Kenner and Ogryzlo's[15] for v=0 of the $c\ ^1\Sigma_u^-$ state, along with measurements from the $A\ ^3\Sigma_u^+$ state from Knutsen *et al.*[14] Where a comparison can be made for O_2 and He, the rate constants are more than a factor of 100 smaller for v=0 than those we measure for v=9. Of course, the v=0 level cannot undergo vibrational cascade, which may be a significant removal process for v=9 with O_2. Also, the v=0 level lies below all other vibrational energy levels of the other two triplet Herzberg states, eliminating the possibility of the relaxation via transfer to the triplet states as might occur in higher vibrational levels. Because of these differences, a direct comparison may be somewhat misleading, since these other pathways may be involved in the removal of the vibrationally excited level. Much faster rate constants are seen for removal of molecules in vibrationally excited levels of the other O_2 singlet states, $b\ ^1\Sigma_g^+$ and $a\ ^1\Delta_g$.[25,26] Large differences between low and high vibrational levels are seen when measurements in the $A\ ^3\Sigma_u^+$ state from this laboratory[4] and the results for the $A\ ^3\Sigma_u^+$ state from Kenner and Ogryzlo[15,27,28] are compared. Difficulties with the indirect experimental method of Kenner and Ogryzlo may also account for the difference.[1,16]

We can also compare the magnitude of the $c\ ^1\Sigma_u^-$ rate constants to those for the $A\ ^3\Sigma_u^+$ state, as shown in Table II. Although the $A\ ^3\Sigma_u^+$ v=6 level lies at only slightly higher energy, we find that for O_2 collisions, the $c\ ^1\Sigma_u^-$ v=9 level relaxes about a factor of 5 slower. While for N_2, the difference is smaller. For He, no rate constant has been measured in v=6 of the $A\ ^3\Sigma_u^+$ state; however, comparing with v=7, the difference for He is smaller still. An experiment that examines the removal from v=5 of the $A\ ^3\Sigma_u^+$ state would be interesting, since it is nearly isoenergetic with $c\ ^1\Sigma_u^-$ v=9 ($\Delta E \sim 90\ cm^{-1}$), and would allow for a more direct comparison of states at similar energies.

These results are extremely important for modeling the O_2 nightglow on earth.[13,14,16–19] Given the relative abundances of N_2 and O_2 on earth, and the relative rate constants, N_2 removal will dominate in our atmosphere for $c\ ^1\Sigma_u^-$ v=9. This relative importance may change at the lower temperature of the mesosphere, so the temperature dependence will also be measured for each collider. In this laboratory, significantly different temperature dependences in v=9 of the $A\ ^3\Sigma_u^+$ state have already been observed for O_2 and N_2 relaxation.[29] As the $c\ ^1\Sigma_u^-$ v=9 vibrational level is at the

TABLE II. Comparison of removal rate constant measurements for O_2 electronic states.[a]

Collider	This work $c\ ^1\Sigma_u^-$, v=9	Kenner and Ogryzlo[15] $c\ ^1\Sigma_u^-$, v=0	Knutsen *et al.*[4] $A\ ^3\Sigma_u^+$, v=6	Knutsen *et al.*[4] $A\ ^3\Sigma_u^+$, v=7
O_2	$(5.2\pm0.6)\times10^{-12}$	3×10^{-14}	$(2.8\pm0.3)\times10^{-11}$	$(3.5\pm0.3)\times10^{-11}$
N_2	$(3.2\pm0.4)\times10^{-12}$	...	$(1.4\pm0.4)\times10^{-11}$	$(2.4\pm1.0)\times10^{-11}$
He	$(7.5\pm0.9)\times10^{-12}$	6×10^{-15}	...	$(1.4\pm0.6)\times10^{-11}$

[a]Units of $cm^3\ s^{-1}$.

high end of those levels populated in the earth's atmosphere, these measurements should be extended to lower vibrational levels. Overlap with the 2+1 ionization of the ground state[18] may limit measurements using the ionization scheme that was successful here, and a new detection technique may be required.

ACKNOWLEDGMENTS

The authors thank the National Aeronautics and Space Administration, Space Physics Division, Ionospheric, Thermospheric, Mesospheric Physics Program (NASW-4621 and NASW-4440) for support of this work. M.E.O. thanks the National Science Foundation for his support through the Research Experience for Undergraduates Program. T.Y. thanks TÜBİTAK for partial support during this research. We thank Tom Slanger, Mark Dyer, Christian Bressler, Eunsook Hwang, and David Huestis for many helpful discussions during the course of this investigation.

[1] D. R. Bates, Planet. Space Sci. **36**, 875 (1988).
[2] G. Herzberg, Can. J. Phys. **30**, 185 (1952).
[3] R. A. Copeland, J. Chem. Phys. **100**, 744 (1994).
[4] K. Knutsen, M. J. Dyer, and R. A. Copeland, J. Chem. Phys. **101**, 7415 (1994).
[5] R. A. Copeland, K. Knutsen, and T. G. Slanger, in *Proceedings of the International Conference on Lasers '93*, edited by V. J. Corcoran and T. A. Goldman (STS, McLean, VA, 1994), p. 318.
[6] T. G. Slanger and R. A. Copeland, in *Progress and Problems in Atmospheric Chemistry*, edited by J. R. Barker (World Scientific, Singapore, 1996), p. 500.
[7] D. L. Huestis, R. A. Copeland, K. Knutsen, T. G. Slanger, R. T. Jongma, M. G. H. Boogaarts, and G. Meijer, Can. J. Phys. **72**, 1109 (1994).
[8] T. G. Slanger and D. L. Huestis, J. Geophys. Res. **86**, 3551 (1981).
[9] W. E. Sharp and D. E. Siskind, Geophys. Res. Lett. **16**, 1453 (1989).
[10] R. W. Eastes, R. E. Huffman, and F. J. LeBlanc, Planet, Space Sci. **40**, 481 (1992).
[11] J. Stegman and D. P. Murtagh, Planet. Space Sci. **39**, 595 (1991).
[12] J. L. Fox, Can. J. Phys. **64**, 1631 (1986).
[13] G. Witt, J. Stegman, B. H. Solheim, and E. J. Llewellyn, Planet. Space Sci. **27**, 341 (1979).
[14] V. A. Krasnopolsky, Planet. Space Sci. **29**, 925 (1981).
[15] R. D. Kenner and E. A. Ogryzlo, Can. J. Chem. **61**, 922 (1983).
[16] D. R. Bates, in *Progress in Atmospheric Physics*, edited by R. Rodrigo, J. J. López-Mereno, M. López-Puertas, and A. Molina (Kluwer Academic, Boston, 1988), p. 3.
[17] D. R. Bates, Planet. Space Sci. **36**, 869 (1988).
[18] J. E. Johnston and A. L. Broadfoot, J. Geophys. Res. **98**, 21593 (1993).
[19] D. R. Bates, in *Progress and Problems in Atmospheric Chemistry*, edited by J. R. Barker (World Scientific, Singapore, 1996), p. 420.
[20] D. A. Ramsay, Can. J. Phys. **64**, 717 (1986).
[21] R. Ogorzalek-Loo, W. J. Marinelli, P. L. Houston, S. Arepalli, J. R. Wiesenfeld, and R. W. Field, J. Chem. Phys. **91**, 5185 (1989).
[22] R. E. Huffman, J. C. Larrabee, and Y. Tanaka, J. Chem. Phys. **40**, 356 (1964).
[23] K. Ito, K. P. Huber, K. Yoshino, M. Ogawa, and Y. Moriok, J. Mol. Spectrosc. **171**, 1 (1995).
[24] J. P. England, B. R. Lewis, S. T. Gibson, and M. L. Ginter, J. Chem. Phys. **104**, 2765 (1996).
[25] T. G. Slanger, Can. J. Phys. **64**, 1657 (1986).
[26] O. Klais, A. H. Laufer, and M. J. Kurylo, J. Chem. Phys. **73**, 2696 (1980).
[27] R. D. Kenner and E. A. Ogryzlo, Int. J. Chem. Kin. **12**, 501 (1980).
[28] R. D. Kenner and E. A. Ogryzlo, Chem. Phys. Lett. **103**, 209 (1983).
[29] E. S. Hwang and R. A. Copeland, Geophys. Res. Lett. (submitted).